



Since January 2020 Elsevier has created a COVID-19 resource centre with free information in English and Mandarin on the novel coronavirus COVID-19. The COVID-19 resource centre is hosted on Elsevier Connect, the company's public news and information website.

Elsevier hereby grants permission to make all its COVID-19-related research that is available on the COVID-19 resource centre - including this research content - immediately available in PubMed Central and other publicly funded repositories, such as the WHO COVID database with rights for unrestricted research re-use and analyses in any form or by any means with acknowledgement of the original source. These permissions are granted for free by Elsevier for as long as the COVID-19 resource centre remains active.



Review

Inactivation of viruses on surfaces by infrared techniques



Baki Karaböce^{a,*}, Evren Saban^a, Ahsen Aydın Büyük^b, Hüseyin Okan Durmuş^a, Rauf Hamid^c, Ahmet Baş^c

^a TÜBİTAK ÜME, Turkey

^b Kocaeli University, Biomedical Faculty, Turkey

^c İstanbul University Cerrahpaşa, Internal Medical Sciences, Turkey

ARTICLE INFO

Index Terms:

Virus transmission
 COVID-19
 SARS-CoV-2
 Infrared
 Inactivation
 Infectious disease
 Phi6 bacteriophage

ABSTRACT

Several studies on vaccines and medicines against virus-based illnesses (COVID-19, SARS, MERS) are being conducted worldwide. However, virus mutation is an issue. Therefore, inactivation and disinfection of viruses are crucial. This paper presents a method for virus inactivation by physical techniques. The infrared (IR) technique is preferred over other disinfection techniques such as ultraviolet (UV) and chemical disinfectants (alcohol) due to the associated health and environmental benefits.

In this study, IR sources with various wavelengths were characterized and a far infrared (FIR) source was used to inactivate viruses. FIR sources have a therapeutic effect on the human body and have been used in medical centers. Virus spread is highly affected by environmental conditions such as temperature, humidity, and airflow. A setup with IR sources, an IR camera, an automatically controlled humidity chamber, and an airflow unit was constructed to study the viability of viruses in stationary droplets as a function of relative humidity and temperature. Bacteriophage *Phi6* was used as a model organism for studying enveloped viruses such as influenza and coronavirus. IR techniques were used for studying virus inactivation. The effect of various physical conditions such as temperature, humidity, and airflows was considered to study the effect of radiation on the stationary droplets of *Phi6*. All measurements were performed under laboratory conditions with controlled temperature and humidity. The IR camera system was used to measure the surface temperature of *Phi6* suspension droplets. The samples subjected to IR radiation were processed for plaque assay preparation and counting. Measurements were carried out to reduce and eliminate droplets, which are one of the transmission pathways of viruses. IR was radiated in closed and open-air conditions with appropriate humidity and temperature.

This study reports the effective inactivation of viruses by FIR. The inactivation rate under 50 %rh for IR radiated at 1.4 m height for 3 h in closed environmental chamber was 90%, and that under an airflow rate of 0.20 m/s for 10 min in open-air conditions at a height of 1.0 m was 45.7%.

1. Introduction

COVID-19 is the disease caused by the new type of coronavirus, SARS-CoV-2. It was first reported in December 2019. It caused an epidemic worldwide and was declared a pandemic by the World Health Organization in March 2020 [1]. According to the WHO, by first quarter of 2022, 5.5 million deaths due to COVID-19 were reported [2–5]. Past outbreaks of SARS and MERS, as well as the recent SARS-CoV-2, show that new epidemics may occur in the future. However, it is essential to ensure that the epidemic is eliminated with minimum adverse situations in these cases. Many factors affect the course of such outbreaks, with climate factors being prominent in the spread of the coronavirus [6–12].

Several studies have investigated the effect of humidity and temperature on the increase and decrease in the transmission rates of infectious diseases with respect to climatic factors. The basic idea here is that humidity and temperature are periodically and seasonally variable, and respiratory viral infections increase or decrease in parallel with this change [13–17]. Previous reports have found that the influenza viruses are more persistent in cold and dry or very humid conditions, as their inactivation rate is low [18,19].

The SARS-CoV-2 virus is not viable outside of a living organism (host). It requires suitable environmental conditions for spreading. Most viruses survive best at both extremely high (84 %rh and above) and low (30 %rh and below) relative humidity (rh) environments but are highly

* Corresponding author.

E-mail address: baki.karabocce@tubitak.gov.tr (B. Karaböce).

<https://doi.org/10.1016/j.ijthermalsci.2022.107595>

Received 16 December 2021; Received in revised form 16 March 2022; Accepted 23 March 2022

Available online 4 June 2022

1290-0729/© 2022 Elsevier Masson SAS. All rights reserved.

degraded, i.e., inactivated, at medium humidity (40 %rh to 60 %rh) [6, 20]. The virus infectivity decreases exponentially as the temperature increases between 14 °C and 34 °C. This suggests the existence of a relationship between virus inactivation and temperature [21].

Infectious diseases can be transmitted from one individual to another by inhalation (aerosol), as a result of sneezing or coughing (droplets), and by contact with the surfaces on which droplets (fomite) exist. These droplets and aerosols contain human respiratory fluid and microorganisms. The respiratory fluid provides the conditions for the virus to remain active. Respiratory fluid from surface droplets or suspended aerosols may evaporate to a certain extent when released in ambient conditions. Water loss in the respiratory fluid and contents such as proteins and sodium chloride cause a change in the ambient conditions. The pH of the environment also changes. It is envisaged that an increase in the concentration of the medium can cause the inactivation of microorganisms. It is also reported that a high temperature causes high inactivation rates [22,23]. Heat treatment applied to viruses increases their inactivation by disrupting their surface proteins; in other words, the viruses become less contagious [24]. One study clearly showed that host cell fluids containing virions contain electrolytes, amino acids, and NaCl. The higher concentration resulting from evaporation leads to faster virus inactivation. Ambient humidity also affects the inactivation rate [25]. Thus, it is well known that humidity and temperature substantially affect the stability of viruses [23,26,27].

Many studies have reported that the decay of viruses outside of the host depends on environmental conditions (humidity, temperature, airflow and evaporation kinetics, etc.). A study aimed to evaluate the relationship between weather factors (temperature, humidity, solar radiation, wind speed, and rainfall) and SARS-CoV-2 infection in the State of Rio de Janeiro, Brazil. Solar radiation showed a strong negative correlation with the incidence of SARS-CoV-2, whereas temperature (maximum and average) and wind speed showed a negative correlation [15]. Our previous study experimentally proved that infrared (IR) radiation could accelerate the drying of droplets by a few orders of magnitude compared to conditions with no IR radiation [28]. Under favorable conditions, the transmission of viruses leads to an increase in the replication rate of viruses on the hosts, resulting in a higher risk of mutations. Therefore, physical methods that can be used safely in indoor areas are urgently required.

The IR technique, which is not harmful to human health and has no side effects, was used in this study for virus inactivation. Although UV and chemical disinfectants such as alcohol are more frequently used for inactivation, we examined the use of the IR technique because it is a healthy method that is used for therapy.

IR heating involves the transfer of thermal energy in electromagnetic waves. The IR source emits radiation with a peak wavelength towards an object. Although every material emits IR radiations above the absolute temperature, the radiations have different efficiencies, wavelengths, and reflectivities. In IR heating applications, the wavelengths range from 0.7 μm to 1.0 mm, and the radiations are called short wave (near IR), medium wave (medium IR), or long (far IR) wave radiations. FIR sources are efficient heaters that heat the surface on which they radiate, without affecting the ambient temperature. Wavelength of our FIR source is approximately 7.9 μm and surface temperature is around 120 °C. In this study, we conducted experiments to investigate how IR radiation affects virus inactivation. The findings will contribute to the development of new physical disinfection systems.

This paper presents an alternative approach to control the transmission of SARS-CoV-2. Although a surrogate for SARS-CoV-2 was used, the results reveal that the decay rate of enveloped viruses such as SARS-CoV-2 outside of the host can be increased using IR radiation. Because SARS-CoV-2 transmission and disease severity appear to depend on the viral load, the accelerated decay of viruses can substantially impact the control of the SARS-CoV-2 pandemic and subsequent pandemics due to respiratory viruses such as influenza in the future.

2. Materials and methods

The enveloped *Phi6* model bacteriophage was used to simulate SARS-CoV-2 viruses. *Phi6* is a dsRNA phage of the Cystoviridae family. It has been suggested as a suitable surrogate for studying enveloped RNA viruses, including SARS coronaviruses. Similar to the SARS-CoV-2 virus, a lipid membrane encompasses it; furthermore, it has spike proteins and has similar size [29]. Bacteriophage *Phi6* (DSM 21518), a model for enveloped RNA viruses such as SARS-CoV-2, was propagated according to the supplier's instructions. Briefly, *Pseudomonas SP* (DSM 21482), the suggested host of *Phi6*, was inoculated in Tryptic Soy Broth (TSB) medium (Merck Millipore) and incubated overnight at 25 °C. 100 μL *Pseudomonas SP* overnight culture and 3 mL TSB soft agar were mixed and overlaid on TSB agar plates. Lyophilized *Phi6* stock on filter paper was placed on agar plates immediately. The leaves were then incubated at 25 °C for 18 h. The top layer of soft agar was scraped into SM Buffer. The mixture of soft agar and TSB medium was shaken at room temperature for 4–5 h. The mixture was then centrifuged at 5000 g for 15 min to pellet down cells. The remaining bacterial cell debris in the supernatant was filtered through a 0.45 μm membrane. The filtrate was collected as *Phi6* stock and stored at 4 °C. The concentration of the *Phi6* stock was 10^8 – 10^9 plaque-forming units (PFU)/mL, which is determined by plaque assay [30–33]. Experiments were carried out in open-air laboratory conditions, as shown in Fig. 1. The humidity-controlled chamber is showcased in Fig. 2. A scaffold system was designed to install IR panels at different positions for ambient conditions (laboratory conditions), as seen in Fig. 1. In this way, it is possible to apply the IR radiation from the desired distances (0.5 m, 1 m, and 1.4 m). During the experiments, the surface temperatures of the plates radiated by IR sources were recorded with an IR camera (Optris PI, accuracy is ± 2 °C). An air fan was used to generate airflow. The plate with *Phi6* droplets was placed on a pan of a precise balance during IR application. A humidity-controlled cabinet with dimensions 1 m \times 1 m \times 1 m was constructed, as seen in Fig. 2. An air nebulizer is used for humidity generation in the cabin whose isolation satisfies stable humidity. A control circuit was used to control and stabilize the required humidity values. During the experiments, the surface temperatures of the plates radiated by IR sources were recorded with an IR camera. Testo 480 Digital Temperature, Humidity and Airflow meter was used with accuracies of 0.1 °C, 0.1 %rh, and 0.01 m/s.

The effect of IR radiation on the viability of the *Phi6* virus in stationary droplets was determined by spotting 50 \times 2 μL droplets with a total volume of 100 μL stock virus suspension in SM buffer on a 35 mm tissue culture plate. The droplet preparation process for the experiment and control plates required approximately 1.5 min. The measurements

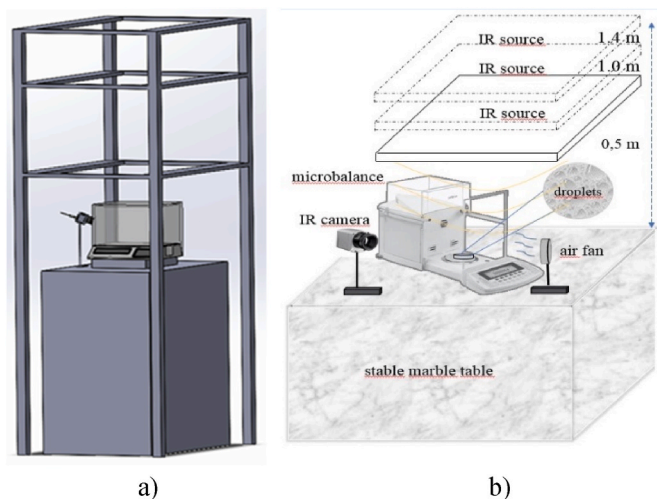


Fig. 1. Experimental setup for measurements in open environment. a) Scaffold system and b) schematic details of the measurement set up.

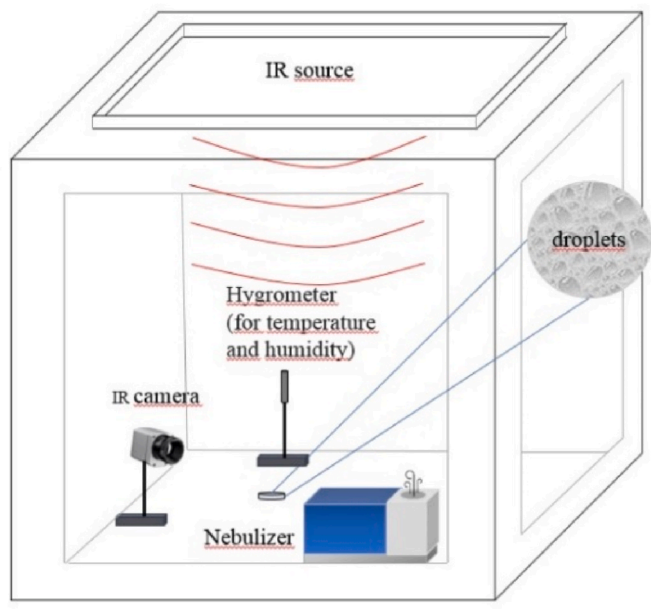


Fig. 2. Experimental set up for the measurements inside the humidity cabin.

were observed with a microbalance before the experiment, and no significant difference was observed between the experimental and control plates. The culture plate was placed on a pan of a precise balance installed on a vibration-free marble block. The balance pan with covers surrounding the half side establishes a controlled and stable environment during IR application. This situation allowed us to compare our previous droplet mass reduction experiments with IR radiation experiments. Placement of the culture plate on the pan of precise balance has created an opportunity to observe the drying and vanishing of the droplets. Humidity, distance, and time dependence of degradation of *Phi6* bacteriophage by IR radiation were examined. Even though we did not work with SARS-Cov2 but *Phi6* bacteriophage, we know the drying mechanism and times of water droplets, which are carriers (environments of viruses) for viruses [28]. FIR sources have been mostly used because of their positive effects on human health. The Near IR and Medium IR were also studied. Kuas ISP Basic450 (600 mm × 600 mm panel) was used as the FIR source, Kuas ISP Basic450 (600 mm × 600 mm panel) was used as the MIR source, and the Kuas I-PIPE (113.5 cm × 20 cm) was used as the NIR source. Kuas ISP Basic450 FIR source was placed on the top of the Culture plate, where droplets were spotted at 0.5 m, 1 m, and 1.4 m heights. While one culture plate with *Phi6* bacteriophage was radiated by FIR source, other equivalent culture plates with *Phi6* bacteriophage were prepared and used as a control solution in the same environment with no IR radiation. As soon as the FIR application had been completed, both samples were quantified and compared by triplicate plaque assay.

Dried virus droplets were collected by adding 1 mL SM Buffer and shaking by gyro rocker for 15 min. 9-Fold serial dilutions of the collected samples were prepared by using SM Buffer. 100 µL of *Phi6* virus serial dilution and 100 µL of *Pseudomonas SP* overnight culture were added to 3 mL soft agar. The mixture is vortexed, poured over hard agar plates, and allowed to solidify. This process is performed for each diluted virus solution obtained by serial dilution, and each is repeated three times. Plates were incubated at 25 °C for 18 h [34]. The number of plaques on plates in which the plaques are between 30 and 300 was counted, and the viral titer of the samples was calculated by the following formula (1) [33]. An appropriate host cell was selected, proper media and growth conditions for cellular and viral viability were prepared, and a viral incubation period for countable plaque formation was accurately determined to improve the accuracy of the plaque assay method

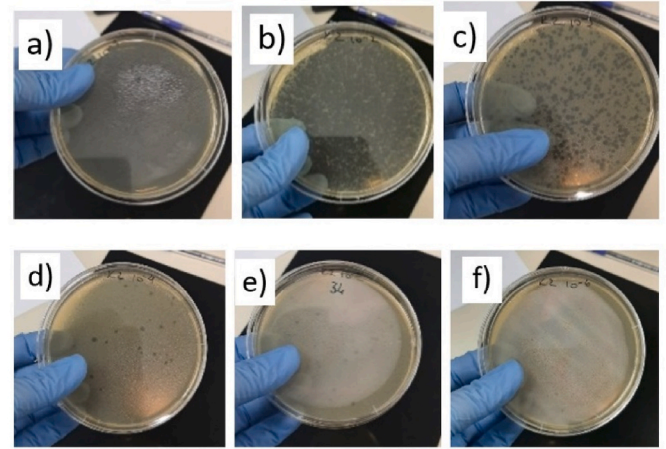


Fig. 3. Images of the formed plaques which represents the lysis of *Phi6* infected bacterial cells observed on plates of all dilution levels. In a), b) and c), plaques are too much that can not be counted, in d) and e) plaques are countable, in f) no significant plaques.

$$\text{Viral Titer (PFU / mL)} = \frac{\text{number of plaques}}{(\text{dilution factor} \times \text{volume of virus dilution added})} \quad (1)$$

[35–37]. To minimize the error in measurements, plaque counting was performed by three different individuals, and the experiments were repeated three times in general. A ± 10% variation in the plaque assay counting technique was achieved [38].

Plaque assay preparation with IR application has been detailed in the supplemental information at the end of the paper.

Images of the formed plaques which represents the lysis of *Phi6* infected bacterial cells observed on plates of all dilution levels are given in Fig. 3 in which plaques are uncountable in a), b) and c), countable in d) and e) but no significant plaques in f). In this experiment, the number of plaques was counted as 262 ± 3 for a dilution of 10^{-8} (Figs. 3d) and 29 ± 1 for 10^{-9} (Fig. 3e). The plate with 262 ± 3 plaques for 10^{-8} dilution was considered for viral titer calculations.

Percent inactivation was calculated after the viral titer in control and IR exposed samples were determined as follows in (2):

$$\% \text{ inactivation} = \left(\frac{\text{Viral Titer}_{\text{Control}} - \text{Viral Titer}_{\text{Exposed}}}{\text{Viral Titer}_{\text{Control}}} \right) \times 100 \quad (2)$$

The time, distance, and airflow dependence of *Phi6* bacteriophage degradation under IR radiation were analyzed in open-air conditions. The humidity, time, and distance dependence were examined.

The uncertainty in the plaque assay experiments was analyzed as tabulated in Table 1. The errors in micropipettes have been presented in a laboratory report by Artel [39]. Other sources of errors were calculated either during observations and experiments or estimated based on previous experiences. The expanded uncertainty of measurement is the product of the standard uncertainty of the measurement multiplied by the coverage factor $k = 2$, which yields a confidence level of approximately 95% for a normal distribution. The standard measurement uncertainty was determined as per GUM and EA-4/02 [40,41]. The expanded uncertainty was calculated as 9.30%. A 10% error was considered for all the measurements.

Airflow value (0.20 m/s) was selected to simulate a flow of a standard fan of air conditioner unit or free airflow in a room at open windows conditions. Humidity levels were chosen to cover the most probable environmental humidity conditions. Humidity levels of 20 % rh–40 %rh represent dry climates or hot indoor areas in winter, 50 % rh–70 %rh represent closed areas in warm seasons, and above 80 %rh represent the conditions in rainy seasons in tropical regions.

Table 1
Uncertainty analysis in plaque assay experiments.

Error sources	Value %	Divisor	Standard uncertainty %
Error in micro pipet (100 µL)	2.24	2.00	1.12
Error in stock virus amount	1.00	1.73	0.58
Error in micro pipet (1 mL)	2.24	2.00	1.12
Volume of virus dilution added	1.00	1.73	0.58
Error in stock virus counting	3.00	1.73	1.73
Time variation before plaque counting	1.00	1.73	0.58
Time and temperature variation in incubation	3.00	1.73	1.73
Distance between IR source and culture plate	0.50	1.73	0.29
Repeatability	6.00	1.73	3.47
Combined Uncertainty			4.65
Expanded Uncertainty (k = 2)			9.30

3. Measurement results

This study used *Phi6* bacteriophage, a pathogenic enveloped virus, and *Pseudomonas Sp*, a propagated host. The experiments were carried out by exposing them to IR radiation at different relative humidity values at different times and distances. The accuracy of maintaining the constant humidity level was kept at approximately 3%. FIR radiation was applied onto droplets of 100 µL infected solution from a distance of 0.5 m for 3 h in a humidity-controlled cabinet. The inactivation rate with respect to various humidity levels is shown in Fig. 4. The increase in moisture content also led to an increase in the inactivation. The lowest percentage of inactivation occurred at 20 %rh and the highest at 80 %rh conditions.

At low humidity levels, droplets dry faster, whereas at higher relative humidity values such as 80 %rh, evaporation becomes slower, and the drying time extends compared to low humidity in the cabin. This parameter will potentially affect the viability of the viruses in the droplets. This can be observed in Fig. 5 in which FIR source was applied at 80 %rh level at a distance of 1 m at different times depending on the time.

Fig. 5 represents the different durations in the cabin at which the FIR radiation was applied at a distance of 1 m at 70 %rh humidity. The increase in FIR application time resulted in higher inactivation, both at 80 %rh and 70 %rh levels.

Inactivation graph of 100 µL virus-containing solution applied for 3 h at a distance of 0.5 m with a FIR source. Error bars indicate the ±10% uncertainty in measurements.

The effect of temperature on virus inactivation has been discussed in

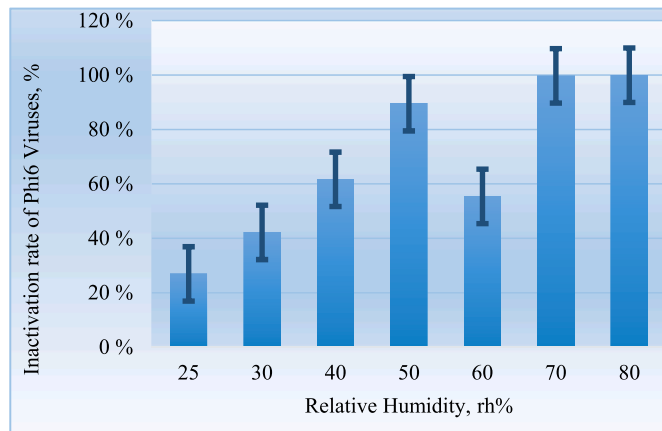


Fig. 4. Inactivation graph of 100 µL virus containing solution applied for 3 h at a distance of 0.5 m with a FIR source. Error bars indicate the ±10% uncertainty in measurements.

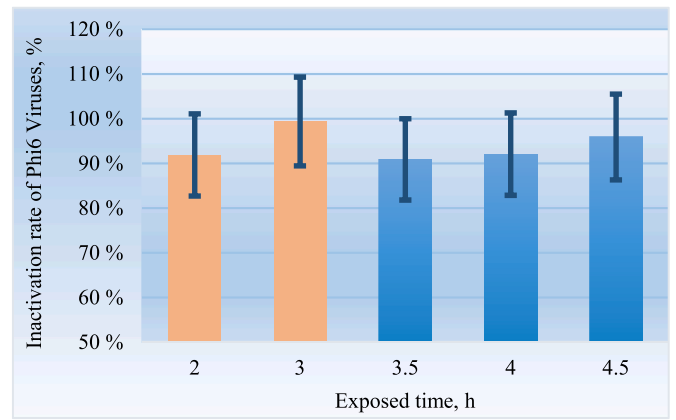


Fig. 5. Graph of the inactivation at different times of FIR application 1 m distance at 80 %rh level (blue columns) and at 70 %rh level (yellow columns). Measurements were performed inside the cabin. Error bars indicate the ±10% uncertainty in measurements.

many studies. For example, in a study they performed between 14 °C and 34 °C, they showed that the virus infectivity decreased exponentially depending on the temperature increase. IR radiation heat surfaces more when applied at close ranges. Depending on this approach, the graphic of the result of the experiment where we used FIR from different distances is shown in Fig. 6. Virus inactivation varies linearly with distance. As the distance decreases, the droplets dry faster, leading to an increase in inactivation. The percentage of inactivation is significantly higher in the experiment performed from 0.5 m distance than the 1 m distance. In addition, the plate’s surface temperature graph contains 100 µL of virus-containing liquid for different humidity levels. The IR radiation is applied for 3 h from a distance of 0.5 m. At all humidity values, the final surface temperatures are between ~40 °C and ~44 °C, as shown in Fig. 7.

To ensure that the initial conditions of all experiments were the same and the IR effect could be seen clearly, the IR heater was activated 3 h before the start of the experiment. Thus, the ambient temperature was stabilized. Therefore, the initial temperatures of the environment for the experiments were the same. After the necessary humidity adjustment was made, the plates containing the droplets were placed in front of the IR heater. These humidity differences also affected the temperature on the surfaces of the plates in the first place. However, as seen in the figure, the final temperatures are approximately the same for all plates.

Experimental results carried out under open-air laboratory conditions are shown in Fig. 8. Virus inactivation higher than 50% has been observed even less than 1 h at 1 m height in open-air laboratory ambient

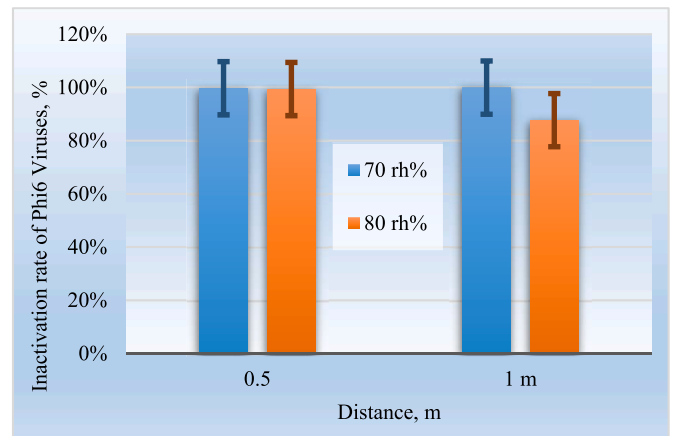


Fig. 6. Virus inactivation in different distances and humidity levels.

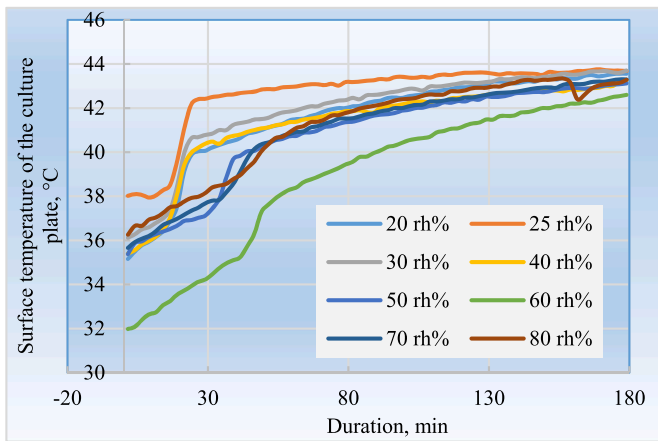


Fig. 7. Surface temperatures of the virus bacteriophage culture plate during IR application. ± 2.0 °C error in surface temperatures measurements should be mentioned.

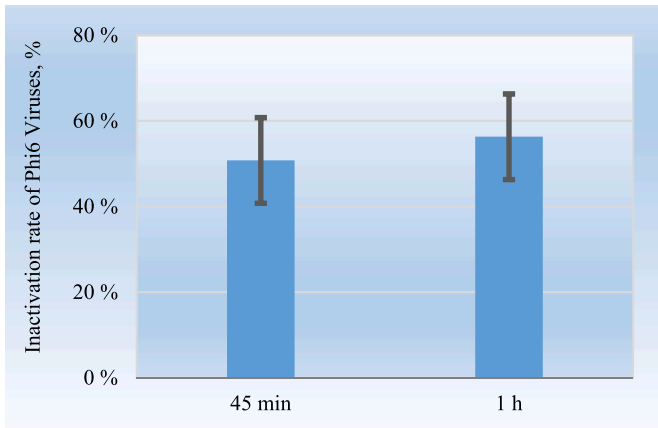


Fig. 8. Virus inactivation according to different application times of the IR application in ambient conditions.

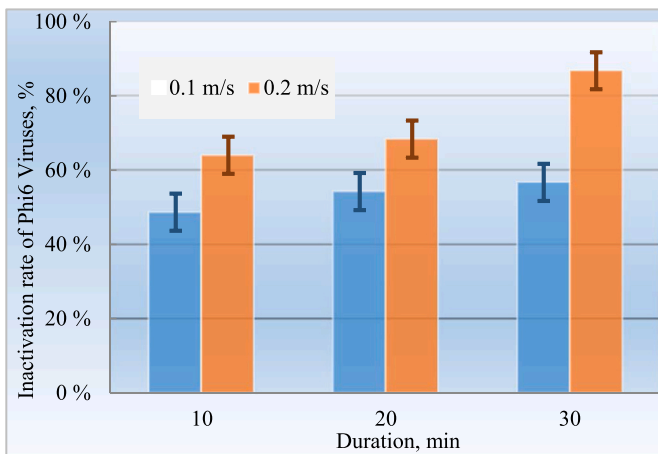


Fig. 9. Virus inactivation with 0.10 m/s (blue columns) and 0.20 m/s (orange columns) air flow in 10 min, 20 min and 30 min of FIR applications. Error bars indicate the $\pm 10\%$ uncertainty in measurements.

conditions. Since the difference in laboratory humidity during the measurement may have prevented the linear measurement with respect to time, the difference between 45 min and 1 h is negligible.

Virus inactivation is even possible in 10 min with 0.20 m/s airflow in open-air conditions. Virus inactivation with 0.10 m/s and 0.20 m/s airflow in 10 min, 20 min, and 30 min of FIR applications can be seen in Fig. 9. Error bars indicate the $\pm 10\%$ uncertainty in measurements.

4. Discussions

Measurements show that IR radiations that induce a temperature rise of above 42 ± 2 °C on the surface affect virus viability on fomites. The heat produced by IR radiation increases the evaporation rate of virus suspension and changes the microscale environment of viruses. We can hypothesize that the higher temperature on the surface leads to a rapid vaporization of the virus suspension droplets; thus, the microscale environment cannot insulate and keep the virus from external changes. At ambient conditions, the microscale environment of the virus would insulate the virus and save the viral structure from surviving and remaining infectious for long periods. A study [42] showed that the droplet evaporation rate changes the solute concentration over time; as water evaporates from the droplets, solutes such as sodium chloride in the media become more concentrated. Inactivation of viruses is governed by the cumulative dose of solutes or the product of concentration and time, as in disinfection kinetics. In addition, another study shows that the lowest virus reduction occurs during evaporation in the presence of the liquid in which the virus is contained. They stated that when the external environment where the virus is completely dried, there will be more concentration increase, and this will cause faster inactivation [25]. However, it will be challenging to establish a connection between the existing humidity and the surface temperature.

Results of studies on preventing virus transmissibility using IR technique were summarized. After the mass reduction measurements under the IR effect, the isotonic fluid that a 3 times faster reduction was achieved, as can be seen partially in our previous study. The impact of mass reduction at various application heights of IR sources is shown in Fig. 10 [28]. The temperature and relative humidity during the measurements are shown in Fig. 11 and Fig. 12, respectively. It must be noted that even though the droplets disappear at temperatures of approximately 35.5 °C, inactivation is possible at temperatures above 42 °C.

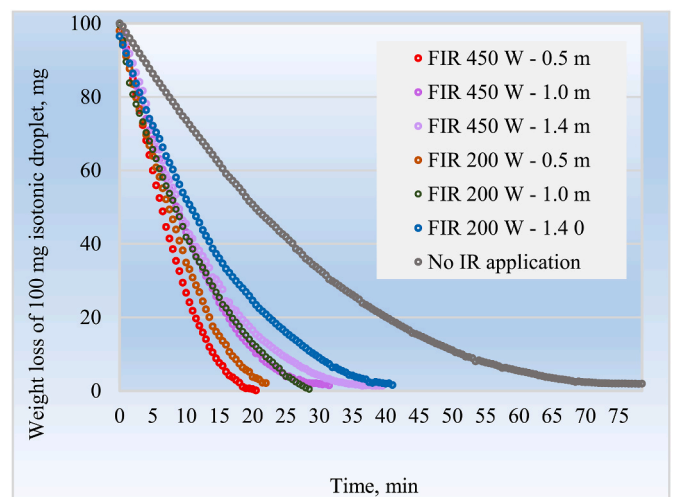


Fig. 10. Time-dependent decrease of 100 mg isotonic droplet under the effect of IR sources and ambient conditions on wooden surfaces. Ambient conditions mean no IR radiation.

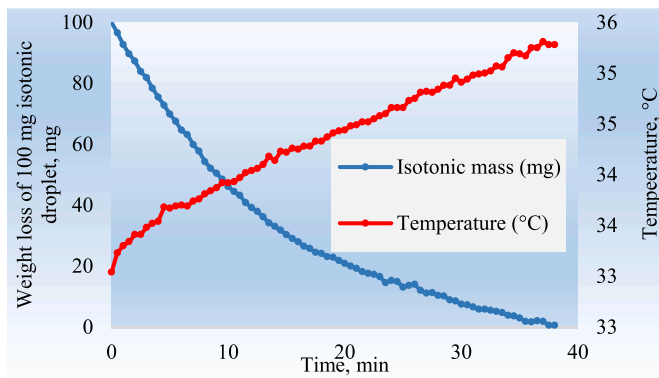


Fig. 11. Temperature during the droplet evaporation by IR application.

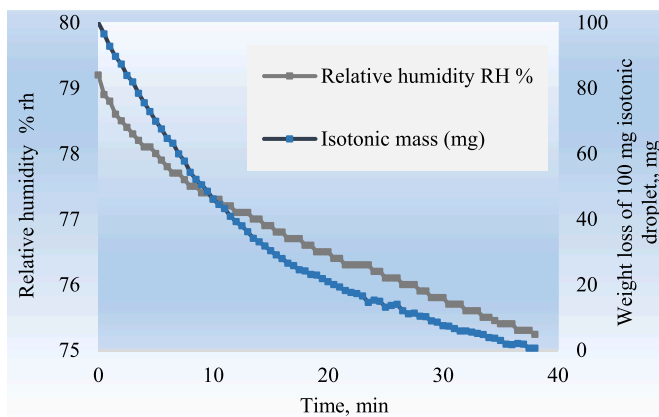


Fig. 12. Relative humidity during the droplet evaporation by IR application.

The discussions below are the results of virus inactivation measurements performed inside a humidity chamber.

In recent studies, the inactivation of many viruses, including various influenza viruses, was lower at 50 %rh–60 %rh humidity. This is consistent with our result. However, studies for investigation of humidity effect on inactivation of viruses are in progress [33,43–45].

IR radiation application was realized on enveloped *Phi6* virus model. Most of the *Phi6* enveloped viruses were inactivated by IR. IR application was made from 0.5 m for 3 h at different humidity levels. Over 90% inactivation was observed at humidity levels above 50 %rh for 100 μ L of the virus suspension. Time-dependent measurements of IR application were performed, and a linear relationship between time and inactivation of viruses was observed for 70 %rh and 80 %rh levels at a height of 1 m. The efficiency of IR radiation in virus inactivation for 70 %rh and 80 %rh levels are higher at 0.5 m than at 1 m. IR radiation has been applied to inactivate the viruses at 80 %rh level according to different application times. Virus solutions were exposed to IR radiation from various distances for 3 h for 80 %rh level. The inactivation rate is significantly higher at 0.5 m compared to 1 m distances. As stated in the studies in the literature, viruses survive best at very low (33 %rh and below) and very high (100 %rh) relative humidity levels and their viability decreases at intermediate level humidity. As a result of low viability, they cannot infect humans, and the risk of transmission is reduced.

Virus inactivation experiments by IR radiation were also realized in open-air conditions besides humidity chamber experiments. Virus inactivation of more than 50% was observed in less than 1 h in room conditions, according to different application times in open-air laboratory conditions. The experimental results showed that virus inactivation in minutes is possible according to data showing that inactivation of viruses is 56.7%, 54.2%, and 48.7% in 30 min, 20 min, and 10 min, respectively.

Even though vaccine and medicine studies are in progress and few SARS-CoV-2 vaccines are in use, the virus can be mutated, and vaccines and medicines may not be effective for viral transmissions. Viruses (and bacteria) have been omnipresent for millions of years. Therefore, preventing viral (and bacterial) transmission is a topic of interest.

Our study shows that IR radiation reduces virus viability. The heat produced by FIR (also MIR and NIR) increases the evaporation rate of the virus suspension and reduces the viral survival rate. The higher the temperature on the surface, the higher the vaporization rate of the virus suspension.

We studied the IR effect on *Phi6* enveloped viruses with bacteriophage (*Phi6-EwB*). We applied IR radiation of various wavelengths on *Phi6* enveloped viruses with bacteriophage. As soon as the IR application ended, *Phi6-EwB* were started to vitalize within minutes. This is not common in real life. Therefore, the degradation of viruses by IR application is more effective than the results declared here. It must be noted that viruses can live only with a convenient medium. Environmental conditions such as above room temperature (23 °C), airflow, and open-air conditions will generally degrade the viruses. Since ASHRAE/ASHRAE Standard 170–2017 in Hospitals states ventilation of between 0.10 m/s and 0.20 m/s for safety and comfortability, we studied the effect of airflow on virus inactivation rate was studied at 0.10 m/s and 0.20 m/s. Time dependence of virus inactivation at various flows showed a linear behavior. Virus inactivation increased with increasing duration of airflow [46].

The membrane and nucleocapsid proteins of viruses such as SARS-CoV-2 are damaged by a temperature increase [47]. To inactivate viruses by thermal methods, temperatures of 60 °C for 30 min, 65 °C for 15 min, or 80 °C for 1 min are considered sufficient. However, this study was carried out in water; therefore, a comparison with the studies conducted in a dry environment is difficult.

For virus inactivation performed by Kampf et al. IR radiation at 60 °C for 30 min can be compared with the partial inactivation when the surface temperature reaches 42 °C in 45 min and 60 min applications seen in Fig. 8, which we obtained from our studies.

For the SARS-CoV-2 in cell culture, 99.99% inactivation was achieved after heating at 56 °C for 15 min, showing that it was compatible with the theoretical model (3) [48].

$$t_4(T) = 1.32^{(37^\circ C - T)} \times 48h \quad (3)$$

In equation (3), t_4 denotes inactivation parameter 4 (4 log10 reductions) and T is the temperature in °C. According to the theoretical model, at a body temperature of 37 °C, 99.99% inactivation occurs in 48 h. In comparison, at 39 °C, 99% inactivation is expected in 14 h and 99.99% inactivation in 28 h. It can be said that the inactivation in the range of 50%–90% obtained at 42 °C for 30 min to 4 h for the MS2 bacteriophage is compatible with the theoretical model (3) developed by Seifer et al. However, it is difficult to make a complete comparison.

5. Conclusion

In this study, a human-friendly FIR source, also known as a therapeutic IR source, was used. Measurements with medium IR and near IR wavelengths were used for comparison. Optimized conditions of FIR usage in closed and partially closed places were determined. The use of FIR led to a decrease in the virus viability and viral transmission by fomites. Virus inactivation is possible within minutes with FIR application in optimized humidity and airflow conditions.

A customized design of FIR (or MIR and NIR) can be used to curb viral transmission by fomites (surfaces of tables, walls, railings, and tools). A general design of FIR can disinfect most viruses (and bacteria). A detailed investigation of the possibly contaminated areas and a custom application of FIR with the help of MIR or NIR can help determine the most effective solution for preventing viral transmission. Since plaque assay experiments are time-consuming, the number of data points

obtained is limited. Hence, future studies will be conducted for detailed airflow measurements.

Various types of prototype FIR devices that simulate the optimum humidity and airflow conditions are in progress in our laboratory. The degradation of viruses is significant for reducing the spread of infections. Moreover, other factors (such as temperature and airflow) can be combined with humidity for the inactivation of viruses. Studies on transmissible gastroenteritis virus (TGEV) and mouse hepatitis virus (MHV) have shown that viral inactivation on surfaces can be realized by different mechanisms [49]. When protein shells (viral capsids) of viruses condense on the boundary surfaces of a solution, the virus surface becomes damaged more easily [50–52]. Drying and interaction at the boundary surfaces can differentiate virus inactivation in different humidity environments. A study showed that at high humidity levels (at around 80 %rh), water molecules evaporate more slowly, hydrophobicity decreases, and inactivation increases at the boundary surfaces [53]. However, further research on this topic is required.

It should be noted that the technique is healthy and may present an additional therapeutic effect. Conventional plaque assay measurements are suitable for determining virus inactivation but are complex and prone to error. Their use in virological experiments is disadvantageous because they require a long time to prepare and process. Therefore, limited data were obtained.

Lastly, this study reported findings from a bacteriophage model, which may not fully represent human viruses. Human viruses, such as influenza virus and coronavirus, should be used in future studies to elucidate the effects of IR exposure on virus survival and transmission.

Declaration of competing interest

The authors declare that they have no known competing financial interests or personal relationships that could have appeared to influence the work reported in this paper.

Data availability

Data will be made available on request.

Acknowledgement

Presented activities have been supported by the framework of the TÜBİTAK COVID-19 projects VirYAP (Reduction of Virus Spread) Project (G1MM-YOG0004) that received funding from the TÜBİTAK ÜME. The authors would like to thank Meltem Aşıcıoğlu for helpful advice, Berkay Somuncu for performing plaque assay experiments, Mihli Nur Bülün and Kadir Ak for performing the measurements.

Appendix A. Supplementary data

Supplementary data to this article can be found online at <https://doi.org/10.1016/j.ijthermalsci.2022.107595>.

References

- [1] Organização Mundial da Saúde, WHO Director-General's Opening Remarks at the Media Briefing on COVID-19 - 11 March 2020, vol. 4, WHO Dir. Gen. speeches, no. March, 2020.
- [2] W. McKibbin, R. Fernando, The Economic Impact of COVID-19, 2020, pp. 45–51.
- [3] R. Baldwin, B.W. di Mauro, Economics in the Time of COVID-19, 2020.
- [4] M. Okereke, et al., Impact of COVID-19 on access to healthcare in low- and middle-income countries: current evidence and future recommendations, *Int. J. Health Plann. Manag.* 36 (1) (2021) 13–17.
- [5] WHO Coronavirus (COVID-19) Dashboard (<https://covid19.who.int/>).
- [6] W. Yang, S. Elankumaran, L.C. Marr, Relationship between Humidity and Influenza A Viability in Droplets and Implications for Influenza's Seasonality, *PLoS One*, 2012.
- [7] K.C. Chong, W. Goggins, B.C.Y. Zee, M.H. Wang, Identifying meteorological drivers for the seasonal variations of influenza infections in a subtropical city - Hong Kong, *Int. J. Environ. Res. Publ. Health* 12 (2) (2015) 1560–1576.
- [8] J. Tamerius, M.I. Nelson, S.Z. Zhou, C. Viboud, M.A. Miller, W.J. Alonso, Global influenza seasonality: reconciling patterns across temperate and tropical regions, *Environ. Health Perspect.* 119 (4) (2011) 439–445.
- [9] D.N. Fisman, Seasonality of infectious diseases, in: *Annual Review of Public Health*, 2007.
- [10] M. Moriyama, W.J. Hugentobler, A. Iwasaki, Annual review of ashvirology seasonality of respiratory viral infections, *Annu. Rev. Virol.* 7 (2020) 1–19.
- [11] M. Moriyama, W.J. Hugentobler, A. Iwasaki, Seasonality of respiratory viral infections, *Annu. Rev. Virol.* 7 (1) (2020) 83–101.
- [12] J. Liu, et al., Impact of meteorological factors on the COVID-19 transmission: a multi-city study in China, *Sci. Total Environ.* 726 (2020) 138513.
- [13] T.P. Loh, et al., Correlations between clinical illness, respiratory virus infections and climate factors in a tropical paediatric population, *Epidemiol. Infect.* 139 (12) (2011) 1884–1894.
- [14] S. Fu, et al., Meteorological factors, governmental responses and COVID-19: evidence from four European countries, *Environ. Res.* 194 (2021) 110596.
- [15] D.K.A. Rosario, Y.S. Mutz, P.C. Bernardes, C.A. Conte-Junior, Relationship between COVID-19 and weather: case study in a tropical country, *Int. J. Hyg Environ. Health* 229 (2020) 113587.
- [16] M. Kanzawa, H. Spindler, A. Anglemeyer, G.W. Rutherford, Will coronavirus disease 2019 become seasonal? *J. Infect. Dis.* 222 (5) (2020) 719–721.
- [17] M. Ahmadi, A. Sharifi, S. Dorosti, S. Jafarzadeh Ghouschi, N. Ghanbari, Investigation of effective climatology parameters on COVID-19 outbreak in Iran, *Sci. Total Environ.* 729 (2020).
- [18] S.F. Dowell, M. Shang Ho, Seasonality of infectious diseases and severe acute respiratory syndrome - what we don't know can hurt us, *Lancet Infect. Dis.* 4 (11) (2004) 704–711.
- [19] F.E.A. Moura, Influenza in the tropics, *Curr. Opin. Infect. Dis.* 23 (5) (2010) 415–420.
- [20] K.A. Kormuth, et al., Influenza virus infectivity is retained in aerosols and droplets independent of relative humidity, *J. Infect. Dis.* 218 (5) (2018) 739–747.
- [21] A.J. Prussin, D.O. Schwake, K. Lin, D.L. Gallagher, L. Buttling, L.C. Marr, Survival of the enveloped virus Phi6 in droplets as a function of relative humidity, absolute humidity, and temperature, *Appl. Environ. Microbiol.* 84 (12) (2018).
- [22] Y.Y. Su, R.E.H. Miles, Z.M. Li, J.P. Reid, J. Xu, The evaporation kinetics of pure water droplets at varying drying rates and the use of evaporation rates to infer the gas phase relative humidity, *Phys. Chem. Chem. Phys.* 20 (2018) 23453–23466.
- [23] L.C. Marr, J.W. Tang, J. Van Mullekom, S.S. Lakdawala, Mechanistic Insights into the Effect of Humidity on Airborne Influenza Virus Survival, Transmission and Incidence, *Journal of the Royal Society Interface*, 2019.
- [24] K.R. Wigginton, B.M. Pecson, T. Sigstam, F. Bosshard, T. Kohn, Virus inactivation mechanisms: impact of disinfectants on virus function and structural integrity, *Environ. Sci. Technol.* 46 (21) (2012) 12069–12078.
- [25] D.H. Morris, et al., The effect of temperature and humidity on the stability of SARS-CoV-2 and other enveloped viruses, *bioRxiv Prepr. Serv. Biol.* (2020), <https://doi.org/10.7554/eLife.65902>.
- [26] K.H. Chan, J.S.M. Peiris, S.Y. Lam, L.L.M. Poon, K.Y. Yuen, W.H. Seto, The effects of temperature and relative humidity on the viability of the SARS coronavirus, *Adv. Virol.* (2011), <https://doi.org/10.1155/2011/734690>.
- [27] M.K. Ijaz, A.H. Brunner, S.A. Sattar, R.C. Nair, C.M. Johnson-Lussenburg, Survival characteristics of airborne human coronavirus 229E, *J. Gen. Virol.* 66 (12) (1985) 2743–2748.
- [28] B. Karaböce, A. Baş, A.A. Büyük, M.N. Bülün, K. Ak, Investigations of degradation of virus spread by physical technique, in: Badnjević, Almir, Gurbeta Pokvić, Lejla (Eds.), *Proceedings of the International Conference on Medical and Biological Engineering, Mostar, Bosnia and Herzegovina, CMBEBIH, 2021, April*, pp. 847–857, 21–24, 2021.
- [29] A. Fedorenko, M. Grinberg, T. Orevi, N. Kashtan, Survival of the enveloped bacteriophage Phi6 (a surrogate for SARS-CoV-2) in evaporated saliva microdroplets deposited on glass surfaces, *Sci. Rep.* 10 (1) (2020 Dec 29) 22419, <https://doi.org/10.1038/s41598-020-79625-z>.
- [30] N. Aquino De Carvalho, E.N. Stachler, N. Cimabue, K. Bibby, Evaluation of Phi6 persistence and suitability as an enveloped virus surrogate, *Environ. Sci. Technol.* 51 (15) (2017) 8692–8700.
- [31] N. Turgeon, M.J. Toulouse, B. Martel, S. Moineau, C. Duchaine, Comparison of five bacteriophages as models for viral aerosol studies, *Appl. Environ. Microbiol.* 80 (14) (2014) 4242–4250.
- [32] D. Verreault, S. Moineau, C. Duchaine, Methods for sampling of airborne viruses, *Microbiol. Mol. Biol. Rev.* 72 (3) (2008) 413–444.
- [33] K. Lin, C.R. Schulte, L.C. Marr, Survival of MS2 and Phi6 viruses in droplets as a function of relative humidity, pH, and salt, protein, and surfactant concentrations, *PLoS One* 15 (12) (2020), e0243505, <https://doi.org/10.1371/journal.pone.0243505>.
- [34] M. Panec, D.S. Katz, Plaque Assay Protocols, American Society for Microbiology, 2006. (Accessed 19 June 2020). Accessed.
- [35] R. Dulbecco, M. Vogt, Some problems of animal virology as studied by the plaque technique, *Cold Spring Harbor Symp. Quant. Biol.* 18 (1953) 273–279.
- [36] A. Baer, K. Kehn-Hall, Viral concentration determination through plaque assays: using traditional and novel overlay systems, *JoVE* 93 (2014) 52065, <https://doi.org/10.3791/52065>. PMID: PMC4255882, PMID: 25407402.
- [37] S. Jane Flint, Lynn W. Enquist, Vincent R. Racaniello, Glenn F. Rall, A. M. Skalka, *Principles of Virology*, fourth ed., vol. 2 Vol.
- [38] S. Payne, *Methods to Study Viruses*, Viruses, 2017, pp. 37–52, <https://doi.org/10.1016/B978-0-12-803109-4.00004-0>. PMID: 1749989.

- [39] Laboratory report 5: Setting Tolerances for Pipettes in the Laboratory, Arte, https://www.artel.co/learning_center/setting-tolerances-for-pipettes-in-the-laboratory/.
- [40] Evaluation of Measurement Data - Guide to the Expression of Uncertainty in Measurement, JCGM 100:2008 GUM 1995 with Minor Corrections, first ed., 2008 Corrected version 2010.
- [41] EA Guidelines on the Expression of Uncertainty in Quantitative Testing, EA-4/16 G:2003, December 2003 rev00.
- [42] K. Lin, L.C. Marr, Humidity-dependent decay of viruses, but not bacteria, in: Aerosols and Droplets Follows Disinfection Kinetics, Environ. Sci. Technol., 2020.
- [43] A.J. Prussin, D.O. Schwake, K. Lin, D.L. Gallagher, L. Buttling, L.C. Marr, Survival of the enveloped virus Phi6 in droplets as a function of relative humidity, absolute humidity, and temperature, Appl. Environ. Microbiol. 84 (2018). No. e00551-18.
- [44] J.R. Songer, Influence of relative humidity on the survival of some airborne viruses, Appl. Microbiol. 15 (1967) 35–42.
- [45] W. Yang, S. Elankumaran, L.C. Marr, Relationship between humidity and influenza A viability in droplets and implications for influenza's seasonality, PLoS One 7 (2012). No. e46789.
- [46] ANSI/ASHRAE/ASHE Standard 170, Ventilation of Health Care Facilities, 2017.
- [47] G. Kampf, A. Voss, S. Scheithauer, Inactivation of coronaviruses by heat, J. Hosp. Infect. 105 (2) (2020). <https://www.ncbi.nlm.nih.gov/pmc/articles/PMC7271332/>.
- [48] S. Seifer, M. Elbaum, Thermal inactivation scaling applied for SARS-CoV-2, Biophys. J. 120 (6) (2021 Mar 16) 1054–1059, <https://doi.org/10.1016/j.bpj.2020.11.2259>, 120.
- [49] L.M. Casanova, S. Jeon, W.A. Rutala, D.J. Weber, M.D. Sobsey, Effects of air temperature and relative humidity on coronavirus survival on surfaces, Appl. Environ. Microbiol. 76 (9) (2010 May) 2712–2717. PMID: PMC2863430, PMID: 20228108.
- [50] S. Thompson, M. Flury, M. Yates, W. Jury, Role of the air-water-solid interface in bacteriophage sorption experiments, Appl. Environ. Microbiol. 64 (1998) 304–309.
- [51] S. Thompson, M. Yates, Bacteriophage inactivation at the air-water-solid interface in dynamic batch systems, Appl. Environ. Microbiol. 65 (1999) 1186.
- [52] T. Trouwborst, S. Kuyper, J.C. de Jong, A. Plantinga, Inactivation of some bacterial and animal viruses by exposure to liquid-air interfaces, J. Gen. Virol. 24 (1974) 155–165.
- [53] J. Mbithi, V. Springthorpe, S. Sattar, Effect of relative humidity and air temperature on survival of hepatitis A virus on environmental surfaces, Appl. Environ. Microbiol. 57 (1991) 1394–1399.